

# Spin-wave resonance in gradient ferromagnets with concave and convex variations of magnetic parameters

Cite as: J. Appl. Phys. **127**, 123903 (2020); <https://doi.org/10.1063/1.5143499>

Submitted: 24 December 2019 . Accepted: 13 March 2020 . Published Online: 30 March 2020

V. A. Ignatchenko , and D. S. Tsikalov



View Online



Export Citation



CrossMark

## ARTICLES YOU MAY BE INTERESTED IN

[Localized spin waves at low temperatures in a cobalt carbide nanocomposite](#)

Journal of Applied Physics **127**, 124301 (2020); <https://doi.org/10.1063/1.5140711>

[Kinetic features for nucleation-growth process of magnetic phase transition in  \$\text{La}\(\text{Fe}\_{0.88}\text{Si}\_{0.12}\)\_{13}\$  compounds](#)

Journal of Applied Physics **127**, 123902 (2020); <https://doi.org/10.1063/5.0002220>

[Effect of anisotropy on phononic band structure and figure of merit of pentamode metamaterials](#)

Journal of Applied Physics **127**, 124903 (2020); <https://doi.org/10.1063/1.5140610>

Lock-in Amplifiers  
up to 600 MHz



# Spin-wave resonance in gradient ferromagnets with concave and convex variations of magnetic parameters

Cite as: J. Appl. Phys. 127, 123903 (2020); doi: 10.1063/1.5143499

Submitted: 24 December 2019 · Accepted: 13 March 2020 ·

Published Online: 30 March 2020



V. A. Ignatchenko<sup>a)</sup>  and D. S. Tsikalov<sup>b)</sup>

## AFFILIATIONS

Kirensky Institute of Physics, Federal Research Center KSC SB RAS, Krasnoyarsk 660036, Russia

<sup>a)</sup>Author to whom correspondence should be addressed: [vignatch@iph.krasn.ru](mailto:vignatch@iph.krasn.ru)

<sup>b)</sup>Electronic mail: [d\\_tsikalov@iph.krasn.ru](mailto:d_tsikalov@iph.krasn.ru)

## ABSTRACT

The theory of spin-wave resonance in gradient ferromagnetic films with magnetic parameters varying in space described by both concave and convex quadratic functions is developed. Gradient structures such as a potential well, a potential barrier, and a monotonic change in potential between the film surfaces for both quadratic functions are considered. The waveforms of oscillations  $m_n(z)$ , the laws of the dependence of discrete frequencies  $\omega_n$ , and relative susceptibilities  $\chi_n/\chi_1^0$  of spin-wave resonances on the resonance number  $n$  are studied. It is shown that the law  $\omega_n \propto n$  for  $n < n_c$ , where  $n_c$  is the resonance level near the upper edge of the gradient inhomogeneity, which is well known for a parabolic potential well, is also valid for the potential barrier and for the monotonic change in potential, if these structures are formed by a concave quadratic function. It is shown that the law  $\omega_n \propto (n - 1/2)^{1/2}$ , which we numerically derived and approximated by the analytical formula, is valid for all three structures formed by a convex quadratic function. It is shown that the magnetic susceptibility  $\chi_n$  of spin-wave resonances for  $n < n_c$  is much greater than the susceptibility of resonances in a uniform film. An experimental study of both laws  $\omega_n(n)$  and  $\chi_n(n)$  would allow one to determine the type of quadratic function that formed the gradient structure and the form of this structure. The possibility of creating gradient films with different laws  $\omega_n(n)$  and the high magnitude of the high-frequency magnetic susceptibility  $\chi_n(n)$  at  $n < n_c$  make these metamaterials promising for practical applications.

Published under license by AIP Publishing. <https://doi.org/10.1063/1.5143499>

## I. INTRODUCTION

Electromagnetic and elastic waves in substances with artificially created smooth inhomogeneities of material parameters—the refractive index and elastic constants, respectively—are intensively studied experimentally and theoretically. A detailed review of the research and use of such metamaterials in application devices is given in the book.<sup>1</sup> The situation with the development of both experimental and theoretical studies of spin waves in gradient magnetic metamaterials is fundamentally different from the situation with the study of electromagnetic and elastic waves. Until recently, theoretical and experimental studies of spin waves in ferromagnets dealt only with the natural gradient inhomogeneity, which arises uncontrollably in the production of thin magnetic films.

Targeted experimental studies of gradient magnetic materials are just a beginning. The authors of Ref. 2 developed a technology for creating layered films in which the magnetic parameters of the

layers smoothly change across the film thickness, simulating a predetermined law of change in the magnetization  $M(z)$  or exchange  $\alpha(z)$ . By appropriate selection of the alloy composition for each layer, the authors obtained samples in which one of the magnetic parameters changes according to a given law, while the others remain approximately constant. The dependence of the parameter on  $z$  obtained with this technology is stepwise, but with small layer thicknesses, it can be approximated by a smooth function. Spin-wave resonance was also studied in Ref. 2 on the obtained gradient samples.

The development of the theory of spin-wave resonance in the natural gradient ferromagnets began in the 1960s. It was stimulated by experimentally discovered deviations of the dependence of the resonance frequencies  $\omega_n$  (or resonance fields  $H_n$ ) on the mode number  $n$ , from the quadratic law  $\omega_n \propto n^2$  predicted by Kittel's theory<sup>3</sup> for homogeneous magnetic films. In Ref. 4, it was assumed

that these deviations are due to the smooth inhomogeneity of the magnetization  $M$  over the film thickness caused by various technological factors. The actual dependences of the magnetization  $M$  on  $z$  were unknown, but there was reason to believe that the function  $M(z)$  decreases from the middle of the film to its surfaces. Therefore, the convex quadratic function  $M(z)$  for modeling was used, which, due to the minus sign in the expression of the demagnetizing field  $H_m(z) = -4\pi M(z)$ , led to a parabolic potential well in the effective magnetic field  $H^{\text{eff}}(z)$ . The approximate linearized equation for spin-wave oscillations in a ferromagnet with  $z$ -dependent magnetization  $M(z)$  or uniaxial magnetic anisotropy  $\beta(z)$  has the form of the Schrödinger equation for electrons in the external potential  $U(z)$ . Exact solutions of these equations for a concave quadratic potential  $U(z)$  (potential well) are expressed in terms of a confluent hypergeometric Kummer function.<sup>5</sup> In some cases, technological factors led to another dependence of  $M(z)$ —its almost linear change from one surface of the film to another. For such cases, the solution of the Schrödinger equation can be expressed in terms of the Airy functions.<sup>5</sup> The characteristics of spin-wave oscillations, taking into account both the features of the magnetic system and the boundary conditions on the film surfaces, were obtained from these exact solutions by approximate analytical, graphical, and numerical methods in Refs. 6–11. The main one of these characteristics is the law of the dependence of discrete frequencies  $\omega_n$  (or resonance fields  $H_n$ ) on the spectral level number  $n$  (number of the spin-wave resonance peak). For frequencies  $\omega_n < \omega_c$ , where  $\omega_c$  corresponds to the upper edge of the gradient potential well, a model with a parabolic dependence of the effective magnetic field  $H^{\text{eff}}$  on  $z$  leads to the law  $\omega_n \propto n$ , and a model with a linear dependence of  $H^{\text{eff}}(z)$  leads to the law  $\omega_n \propto (n - 3/4)^{2/3}$ , where  $n = 1, 2, 3, \dots$ . For frequencies  $\omega_n > \omega_c$ , the dependence of  $\omega_n$  on  $n$  with increasing  $n$  for both models approaches the law  $\omega_n \propto n^2$ , which corresponds to a uniform film.

Theoretical works<sup>6–11</sup> made it possible to qualitatively explain the results of experimental studies of spin-wave resonance of those years and stimulated an improvement in the technology for producing films. An increase in technological requirements (high vacuum, temperature conditions, artificial formation of boundary conditions, etc.) led to the creation of more advanced permalloy films,<sup>12</sup> for which Kittel's law  $\omega_n \propto n^2$  was well satisfied for all values of  $n$ . However, deviations from this law for frequencies  $\omega_n < \omega_c$  are still observed both on films of alloys other than in Ref. 12 and on films of granular materials consisting of small ferromagnetic particles in a non-magnetic matrix. These deviations are qualitatively explained by the authors of experimental works in the framework of models of either a parabolic<sup>13–19</sup> or linear<sup>11,20–24</sup> variation of the effective magnetic field.

In Refs. 6–11, spin-wave modes were calculated only for two functions  $M(z)$ , the spontaneous appearance of which in the sprayed films is most likely: parabolically decreasing from the center of the film to its surfaces and linearly dependent on  $z$ . After the development of technology for the artificial creation of gradient films in which magnetic parameters vary according to a predetermined law,<sup>2</sup> it became clear that many different profiles of changes in magnetic parameters along the  $z$  coordinate can be realized. Of particular interest is the possibility shown by the authors of Ref. 2 to create films in which only one of the magnetic parameters changed according to a given law, while the others remained

approximately constant. The one-dimensional wave equations in this case contain one coordinate-dependent coefficient, the profile of which is described by some function  $U(z)$ . The development of the theory of waves in such a gradient material involves, in the general case, a sequential solution of two problems: (i) finding the exact solution of the differential equation with a coordinate-dependent coefficient and (ii) analyzing this exact solution in relation to a specific physical model using approximate analytical or numerical methods. Such a program was implemented in our work,<sup>25</sup> in which the method of searching for the profiles of the gradient dependence of the material parameters of matter on the coordinates, which allows one to obtain an exact solution of the wave equations developed earlier for electromagnetic and elastic waves,<sup>1</sup> is generalized to the case of spin waves in gradient ferromagnets. The found profiles and the obtained exact solutions were then used in the same work to develop the theory of spin-wave resonance in a ferromagnet with space-changing parameters of uniaxial magnetic anisotropy  $\beta(z)$  and exchange  $\alpha(z)$ . However, the first, purely a mathematical problem, has already been solved in many cases: exact solutions of differential equations with coordinate-dependent coefficients are well known for a number of profiles of these coefficients.<sup>5</sup> In these cases, the primary problem of the theory of spin waves is the use of this exact solution to calculate the spectrum and amplitudes of standing spin-wave oscillations in thin magnetic films. We are dealing in this work with just such a situation.

The goal of this work is to develop the theory of spin-wave resonance for quadratic gradient structures of the form of a potential well, a potential barrier, and a monotonic change in the magnetic parameters from one surface of the film to another. We study the potentials described both by ordinary concave (increasing with  $z$  growth) and convex (decreasing with  $z$  growth) quadratic functions.

## II. GRADIENT MAGNETIC STRUCTURES AND THE EQUATION OF MOTION

We consider the case of spin-wave resonance in an external constant magnetic field  $H$  directed along the  $z$  axis perpendicular to the film surface. The axis of the uniaxial anisotropy is also directed along the  $z$  axis. In a gradient film, when the effective magnetic field along the film thickness is a function of the  $z$  coordinate, the approximate equation of motion for the resonant circular projection of the magnetization  $m(z, t)$  has the form<sup>6–11</sup>

$$\frac{d^2 m}{dz^2} + \frac{1}{\alpha M_0} \left[ \frac{\omega}{g} - H^{\text{eff}}(z) \right] m = 0. \quad (1)$$

Here,  $\alpha$  is the exchange parameter,  $M_0 = \langle M(z) \rangle$  is the average magnetization value,  $\omega$  is the frequency, and  $g$  is the gyromagnetic ratio.

Variations in the effective magnetic field  $H^{\text{eff}}(z)$  can be caused either by a dependence on the  $z$  coordinate of either the magnetization  $M(z)$  or the uniaxial anisotropy  $\beta(z)$ ,

$$H^{\text{eff}}(z) = H - [4\pi - \beta(z)]M(z) - \alpha \frac{d^2 M(z)}{dz^2}. \quad (2)$$

Here, the dependence of the magnetization on  $z$  is left only in the expression for  $H^{\text{eff}}(z)$  and is replaced by the average value of

$M_0 = \langle M(z) \rangle$  in the coefficient in front of the term in square brackets of Eq. (1). Estimates show that such a replacement does not lead to significant deviations of the solution from the exact result obtained by numerically solving Eq. (1). We consider cases of variations of  $M(z)$  and  $\beta(z)$  separately: a variable  $M(z)$  at  $\beta = \text{const}$  and a variable  $\beta(z)$  at  $M = \text{const}$ . The last term in Eq. (2) is a constant value for the quadratic potential.

We consider the case when the magnetization  $M(z)$  depends on  $z$ . Several gradient structures can be described by the quadratic function  $M(z)$ , six of which are shown in Fig. 1. The solid curves correspond to the convex quadratic function  $M(z)$  or the separated parts of this function. They describe cases where the magnetization decreases quadratically from the middle of the film to its surfaces (a), from the surfaces of the film to its middle (b), and from one surface to another (c). The theory of spin-wave resonance was previously developed only for one of these structures—the structure in Fig. 1(a) described by a solid curve.<sup>6–9</sup> The magnetization  $M(z)$  corresponding to a convex quadratic function can be represented for the gradient structure in Fig. 1(a) in the form

$$M(z) = M_{\max} [1 - \epsilon(pz)^2] \tag{3}$$

and for the gradient structure in Fig. 1(b),

$$M(z^\pm) = M_{\max} [1 - \epsilon(pz^\pm)^2], \tag{4}$$

where  $-d/2 \leq z^- \leq 0, 0 \leq z^+ \leq d/2$ . Here,  $d$  is the film thickness,  $p = 2/d$ ,

$$\epsilon = \frac{\Delta M}{M_{\max}}, \quad \Delta M = M_{\max} - M_{\min}, \tag{5}$$

$$z^\pm = z \pm d/2. \tag{6}$$

The gradient structure in Fig. 1(c), corresponding to a monotonic change in the magnetization  $M(z)$  from one surface of the film to

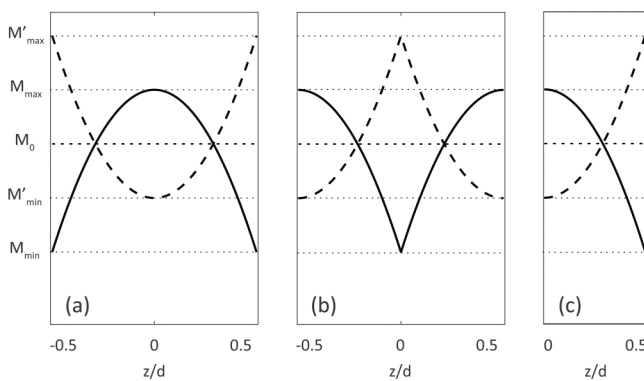


**FIG. 1.** Gradient magnetization structures for convex (thick solid curves) and concave (thick dashed curves) quadratic functions  $M(z)$  with the same mean value  $M_0 = \langle M(z) \rangle$ . The minimum ( $M_{\min}$  and  $M'_{\min}$ ) and maximum ( $M_{\max}$  and  $M'_{\max}$ ) values of the convex and concave quadratic functions  $M(z)$ , respectively (thin dotted lines).

another, is shown for a film whose thickness is half that of the films of structures (a) and (b). This is done for the convenience of comparing the spectral characteristics of all three structures. The magnetization for the structure (c) is described by Eq. (3), in which  $d/2$  now corresponds to the total film thickness. The magnetization  $M(z)$  corresponding to a concave quadratic function (dashed curves in Fig. 1) is described by equations similar to Eqs. (3) and (4) with the replacement of  $M_{\max}$  by  $M'_{\min}$  and the minus sign by the plus sign in square brackets. The magnetization  $M(z)$  appears in the effective magnetic field  $H^{\text{eff}}(z)$  with a negative sign. Therefore, the convex function  $M(z)$  leads to a concave gradient of the magnetic potential  $H^{\text{eff}}(z)$  and vice versa. For example, the previously studied case of a quadratic decrease in the magnetization to the film surfaces<sup>6–9</sup> [Fig. 1(a), a solid convex curve  $M(z)$ ] leads to a concave quadratic potential  $H^{\text{eff}}(z)$ —a potential well. We consider separately the cases of concave and convex quadratic potential.

### A. Concave quadratic potential

Consider the case of variable magnetization  $M(z)$ . Gradient structures corresponding to a concave quadratic potential are described by Eqs. (3)–(6). We represent  $H^{\text{eff}}(z)$  as

$$H^{\text{eff}}(z) = H_0^{\text{eff}} - \Delta H^{\text{eff}}(pz)^2, \tag{7}$$

where

$$H_0^{\text{eff}} = H_0 - (4\pi - \beta + 2\alpha\epsilon p^2)M_{\max}, \tag{8}$$

$$\Delta H^{\text{eff}} = \epsilon(4\pi - \beta)M_{\max}. \tag{9}$$

Equation (1) can be represented in the form

$$\frac{d^2 m}{d\zeta^2} + \left[ \Omega - \frac{1}{4}\zeta^2 \right] m = 0 \tag{10}$$

for all three structures corresponding to such a potential [Figs. 1(a)–1(c), solid curves]. Here, the dimensionless frequency  $\Omega$  and the dimensionless coordinate  $\zeta$  are given by

$$\Omega = \frac{1}{2} (\Delta H^{\text{eff}} p^2 \alpha M_0)^{-1/2} \left( \frac{\omega}{g} - H_0^{\text{eff}} \right), \tag{11}$$

$$\zeta = \sqrt{2} \left( \frac{\Delta H^{\text{eff}}}{p^2 \alpha M} \right)^{1/4} pZ,$$

where  $p = 2/d, Z = z$  for cases (a) and (c), and  $Z = z^\pm$  for case (b). Equation (10) takes the form of the well-known Schrödinger equation for the harmonic oscillator, and its general solution can be represented in the form of parabolic cylinder functions (Weber functions), which are expressed in terms of confluent hypergeometric functions  $M(a, b, c)$  (Kummer functions).<sup>5</sup> The even and odd harmonics of spin waves have the form, respectively,

$$m^s = \exp\left(\frac{-\zeta^2}{4}\right) M\left(-\frac{Q}{2} + \frac{1}{4}, \frac{1}{2}, \frac{\zeta^2}{2}\right), \tag{12}$$

$$m^a = \zeta \exp\left(\frac{-\zeta^2}{4}\right) M\left(-\frac{Q}{2} + \frac{3}{4}, \frac{3}{2}, \frac{\zeta^2}{2}\right), \quad (13)$$

where  $Q$  plays the role of a dimensionless “wave number.” Substitution of Eq. (12) or Eq. (13) into Eq. (10) leads to the dimensionless dispersion law,

$$\Omega = Q, \quad (14)$$

identical for all three structures of Figs. 1(a)–1(c).

We consider solutions, Eqs. (12) and (13), with boundary conditions as pinned,

$$m(z)|_{z=\pm d/2} = 0, \quad (15)$$

or unpinned,

$$\left.\frac{dm(z)}{dz}\right|_{z=\pm d/2} = 0, \quad (16)$$

oscillations on both surfaces of the film. For the magnetic structure of Fig. 1(b), in addition to the boundary conditions of Eq. (15) or Eq. (16), it is also necessary to fulfill the conjugation conditions for the solutions obtained for  $z^+$  and  $z^-$  in the center of the film at  $z = 0$ ,

$$\begin{aligned} m(z^+)|_{z=0} &= m(z^-)|_{z=0}, \\ \left.\frac{dm(z^+)}{dz^+}\right|_{z=0} &= \left.\frac{dm(z^-)}{dz^-}\right|_{z=0}. \end{aligned} \quad (17)$$

This value of  $z$  corresponds to  $z^+ = -d/2$  and  $z^- = d/2$ . Substituting the boundary conditions Eq. (15) or Eq. (16) into Eqs. (12) and (13), we obtain transcendental dispersion equations for finding a discrete set of  $Q_n$  values that were studied numerically.

For numerical studies, we choose magnetic parameters close to real experimental samples:  $\alpha = 2 \times 10^{-12} \text{ cm}^2$ ,  $M_0 = 1000 \text{ G}$ ,  $H_0^{\text{eff}} = 2333 \text{ Oe}$ ,  $\Delta H_0^{\text{eff}} = 5000 \text{ Oe}$ ,  $\omega/g = 3280 \text{ G}$ , and  $d = 300 \text{ nm}$ . The discrete eigenfrequencies  $\Omega_n$ , according to Eq. (14), correspond to the obtained functions  $Q_n$  of  $n$ . Discrete resonant frequencies  $\omega_n$  at  $H = \text{const}$  or discrete resonant magnetic fields  $H_n$  at  $\omega = \text{const}$  can now be found from Eq. (11). It is convenient for us to carry out further analysis in terms of discrete frequencies  $\omega_n$  at  $H = \text{const}$ . Some features of another situation,  $H_n$  at  $\omega = \text{const}$ , will be discussed below when discussing the results of work.

The calculated levels of the discrete frequency spectrum  $\omega_n$  are shown in Fig. 2 (dotted horizontal lines). The waveforms  $m_n(z)$  of the spin-wave unpinned (a)–(c) and pinned (a')–(c') oscillations are also shown in Fig. 2. They are arbitrarily located at the corresponding spectral levels  $n = 1, 2, 3, \dots$ . Black-coated modes correspond to symmetrical and green thin dashed curves to antisymmetric oscillations. The oscillation amplitudes at all levels are normalized to the same value. The forms of the gradient potential for each of the structures are shown by red thick curves. The critical frequency  $\omega_c$  corresponds to the upper edge of the gradient inhomogeneity of the potential. The properties of oscillations at frequencies  $\omega_n < \omega_c$  differ significantly from the waveform of oscillations at frequencies

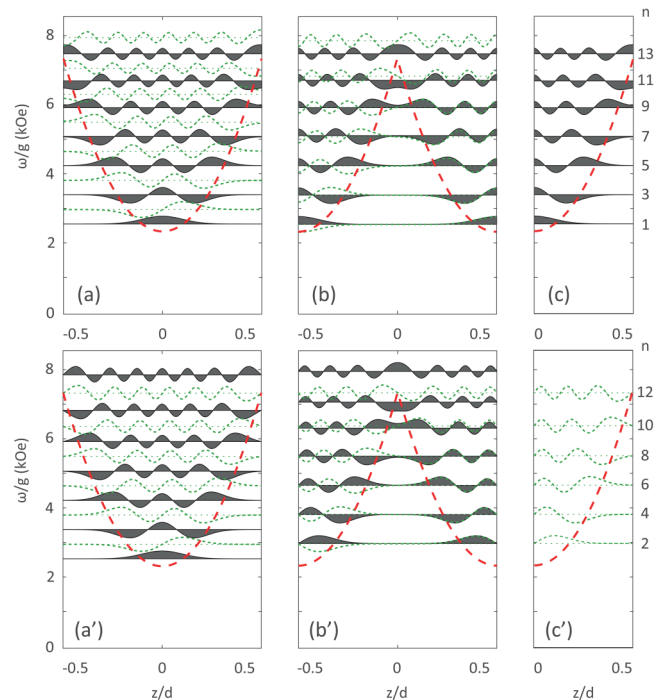


**FIG. 2.** Gradient structures of the effective magnetic field  $H^{\text{eff}}(z)$  described by a concave quadratic function (red thick dashed curves): potential well (a) and (a'), potential barrier (b) and (b'), and monotonic growth of potential between surface films (c) and (c') for unpinned (a)–(c) and pinned (a')–(c') oscillations. Frequencies  $\omega_n$  of discrete levels  $n$  (thin green dotted lines). Black-coated modes correspond to symmetric ones, and green thin dashed curves correspond to the antisymmetric waveform of oscillations  $m_n(z)$ .

$\omega_n > \omega_c$  occurring in a rectangular potential well formed by the surfaces of the film. We will call the critical level  $n = n_c$  whose frequency is closest to  $\omega_c$  from the low frequency side. As can be seen from Fig. 2, the waveform of the oscillations for  $n \leq n_c$  differs significantly from the harmonic one: the effective “wavelength” of oscillations of the confluent hypergeometric function increases as they approach the surface of the gradient potential. For  $n \leq n_c$ , the pinning of the ends of magnetic oscillations on the “surface” of the potential takes place, which was first discovered for films with a parabolic gradient in Ref. 9 and called there “dynamic pinning.” Due to this effect, the waveform at levels  $n \leq n_c$  for films with a parabolic gradient does not depend on the boundary conditions on the film surface [compare Figs. 2(a) and 2(a')].

There are no oscillations outside the potential well, with the exception of tails of internal oscillations penetrating through the potential surface as a result of tunneling. In the case of a potential barrier [Figs. 2(b) and 2(b')], the oscillations at  $n \leq n_c$  occur in two potential wells bounded by the boundaries of the barrier and the corresponding film surfaces. There are no oscillations inside the barrier, with the exception of tails of external oscillations penetrating through the barrier surface as a result of tunneling. In the thin part of the barrier ( $n = 7-11$ ), these tails can merge, forming

transparency windows in the barrier. The sharp difference between the spectrum for the potential barrier and the spectrum for the potential well is that the spectral levels of symmetric and antisymmetric oscillations in the case of a barrier degenerate at levels from  $n = 1$  to  $n = 7$ . This degeneracy is lifted for higher levels. The frequency spectrum  $\omega_n$  and the waveform of spin-wave oscillations in gradient structures in which one of the sides of the potential well(s) is the surface of the film [Figs. 2(b), 2(b'), 2(c), and 2(c')] is substantially determined by the boundary conditions on this surface. The frequencies of unpinned oscillations for the gradient barrier (b) and for the potential well (a) coincide with each other both for  $n < n_c$  and  $n > n_c$ . They correspond to odd levels  $n = 1, 3, 5, \dots$ . The frequencies  $\omega_n$  of the pinned oscillations for the gradient barrier (b') coincide with the frequencies of the antisymmetric oscillations in the potential well (a'), which correspond to even levels  $n = 2, 4, 6, \dots$ . Gradient structures (c) and (c'), corresponding to a monotonic change in the magnetization  $M(z)$  from one surface of the film to another, are shown for a film whose thickness is half the thickness of the films of structures (a) and (b). This is done for the convenience of comparing the spectral characteristics of all three structures. The waveform of oscillations of the structures (c) and (c') is described by the right half of the symmetric function [Eq. (12) for  $z > 0$ ] for unpinned oscillations at  $n = 1, 3, 5, \dots$  (c) and the right half of the antisymmetric function [Eq. (13)] for pinned oscillations at  $n = 2, 4, 6, \dots$  (c'). The index of spectral levels  $n$  chosen in the work corresponds to  $n$  of “half-waves” of oscillations for the gradient structures (a), (a'), (b), and (b') and  $n/2$  of “half-waves” for structures (c) and (c'). If both the wavelength and the penetration depth of the exciting external high-frequency field are much larger than the film thickness, then it can be considered as the value of  $h_0$  independent of  $z$ . In this case, the high-frequency magnetic susceptibility of the  $n$ th oscillation is

$$\chi_n = \frac{1}{h_0 d} \int_{-d/2}^{d/2} m_n(z) dz. \quad (18)$$

Antisymmetric modes are not excited by the field  $h_0$  in either a uniform or gradient film, since for them the integral in Eq. (18) is equal to zero. Symmetric oscillations in a homogeneous film are excited by the field  $h_0$  only for the boundary conditions for pinning oscillations on the film surface [Eq. (15)]. Symmetric modes of the gradient structures (a), (a'), (b), and (b'), in contrast to this, are excited at  $n < n_c$  both with the boundary conditions of pinning, Eq. (15), and unpinning, Eq. (16), on the film surface. This is due to the effect of the dynamic pinning of oscillations inside the film on the “surface” of the gradient potential. The same effect also occurs for the modes of asymmetric structures (c) and (c'). The waveform of the oscillations at the levels  $n > n_c$  with increasing  $n$  is increasingly approaching the harmonic one, for which the conditions of excitation by a uniform along  $z$  a.c. field are preserved only for spins pinned on the film surface [Figs. 2(a')–2(c')].

The main characteristics of the oscillations calculated by us, which can be measured experimentally, are shown in Fig. 3. This is the discrete frequency spectrum  $\omega_n(n)$  [Figs. 3(e)] and 3(e') and relative susceptibility  $\chi_n/\chi_1^0$  [Figs. 3(f) and 3(f')], where  $\chi_1^0$  is the susceptibility of the first peak of a homogeneous film. The same

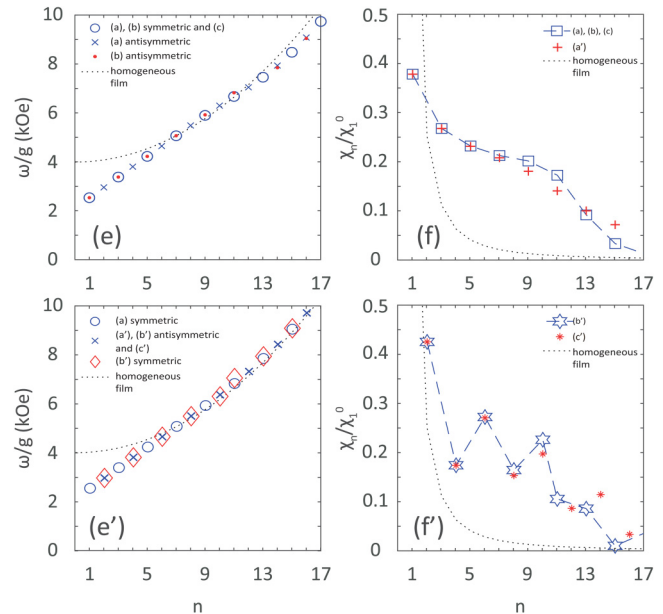


FIG. 3. The frequency spectrum  $\omega_n$  (e) and (e') and the relative susceptibility  $\chi_n/\chi_1^0$  (f) and (f') vs  $n$  for unpinned (e) and (f) and pinned (e') and (f') oscillations in gradient structures of  $H^{\text{eff}}(z)$  described by a concave quadratic function. Designations of the symmetry of oscillations and gradient structures corresponding to them are shown in the figures with links to Figs. 2(a)–2(c) and 2(a')–2(c').

functions calculated by us for a uniform film are also given for comparison (dotted curves). As can be seen from Figs. 3(e) and 3(e'), the points of the discrete laws  $\omega_n(n)$  for all the gradient structures shown in Fig. 2 are located along the same continuous curve. This allows us to make a general conclusion,

The form of the law  $\omega_n(n)$  is the same for all gradient structures in which potential wells are described by a concave quadratic function, or one side of each well is described by a concave quadratic function and the other is bounded by a vertical line (film surface). The “macroscopic” appearance of the gradient structures containing these potential wells does not matter: it can be a potential well [Figs. 2(a) and 2(a')], a potential barrier [Figs. 2(b) and 2(b')], or a monotonous increasing potential [Figs. 2(c) and 2(c')].

The law  $\omega_n(n)$  in the limiting case  $n \ll n_c$  can be written in an analytical form. The form of solutions of Eqs. (12) and (13) for a parabolic potential in an unlimited space is greatly simplified.<sup>5</sup> They can be written in the form of Hermite polynomials, to which the linear law of dependence of  $\omega$  on  $n$  corresponds. It was shown in Refs. 6–9 that this law is the limiting case for  $n \ll n_c$  for the dependence of  $\omega$  on  $n$  in a parabolic potential well in a thin magnetic film [Figs. 2(a) and 2(a')]. The graphs calculated by us [Figs. 3(e) and 3(e')] show that this is also true for all gradient structures shown in Figs. 2(b), 2(b'), 2(c), and 2(c'). Consequently, the law  $\omega_n(n)$  for all gradient structures described by a concave quadratic function, in the limiting cases of small and large  $n$ , has

the form

$$\omega_n \propto \begin{cases} n, & n \ll n_c, \\ n^2, & n \gg n_c. \end{cases} \quad (19)$$

The signs “much smaller” and “much larger” here have a conditional meaning, since the transition between the limiting cases is rather narrow and occurs almost at a distance between two or three levels  $n$  adjacent to  $n_c$ . The points of discrete laws  $\omega_n(n)$  for all gradient structures corresponding to symmetric and antisymmetric oscillations are located along the same continuous curve in different ways for different structures and different boundary conditions. Therefore, the frequencies of antisymmetric oscillations in a potential well [Fig. 3(e), crosses] are located between the frequencies of symmetric oscillations (circles); antisymmetric oscillations in the structure of the potential barrier [Fig. 3(f), red dots] coincide with the frequencies of symmetric oscillations for  $n < n_c$  and are located between the latter for  $n > n_c$ . The frequencies of degenerate oscillations in the structure of the potential barrier in the absence of pinning coincide with the frequencies of symmetric oscillations in the potential well and with the frequencies of antisymmetric oscillations under the boundary conditions of pinning of oscillations.

The relative susceptibilities  $\chi_n/\chi_1^0$  of unpinned oscillations in all gradient structures corresponding to Figs. 2(a)–2(c) are shown in Fig. 3(f) (squares). Here, the susceptibility of the pinned oscillations in the potential well is shown too [Fig. 3(f), crosses]. Both of these functions for  $n < n_c$  coincide with each other and slightly differ from each other for  $n > n_c$ . It is seen that the susceptibility of the first peak of the gradient films is less than the susceptibility of homogeneous films (dotted curve). However, it decreases with increasing  $n$  much slower than the susceptibility of homogeneous films and exceeds the latter by several times for peaks in the range from  $n = 2$  to  $n = n_c + 2$ . The laws of the dependence of  $\chi_n/\chi_1^0$  on  $n$  for the pinned oscillations in the structures of the gradient barrier [Fig. 3(f'), asterisks] and monotonically growing quadratic potential [Fig. 3(f'), blue dots] also coincide for  $n < n_c$  and differ for  $n > n_c$ . Both of these laws are fundamentally different from the laws of Fig. 3(f) for unpinned oscillations in the same structures. The sharp failures of the function  $m_n(z)$  occur at levels 4, 8, and 12, which correspond to an even number of half-waves in each potential well on both sides of the barrier [Fig. 2(b')] and in the potential well of a monotonically increasing potential [Fig. 2(c')]. An even number of half-waves for a harmonic function would lead to a vanishing of the susceptibility, and for degenerate hypergeometric functions, only partial compensation of positive and negative “half-waves” occurs.

### B. Convex quadratic potential

Equation (1) in this case can be represented in a form that differs from Eq. (10) only by the plus sign in square brackets,

$$\frac{d^2 m}{d\zeta^2} + \left[ \Omega + \frac{1}{4} \zeta^2 \right] m = 0. \quad (20)$$

The general solution of this equation can be represented in the form of functions of a parabolic cylinder (Weber functions) of an imaginary argument.<sup>5</sup> The symmetric  $m_s(\zeta)$  and antisymmetric

$m_a(\zeta)$  solutions of Eq. (20) in this case have the form, respectively,

$$m^s = \exp\left(\frac{-i\zeta^2}{4}\right) M\left(\frac{iQ}{2} + \frac{1}{4}, \frac{1}{2}, \frac{i\zeta^2}{2}\right), \quad (21)$$

$$m^a = \zeta \exp\left(\frac{-i\zeta^2}{4}\right) M\left(\frac{iQ}{2} + \frac{3}{4}, \frac{3}{2}, \frac{i\zeta^2}{2}\right). \quad (22)$$

Confluent Kummer hypergeometric functions of an imaginary argument  $M(ia, b, ic)$  in Eqs. (21) and (22) are well studied.<sup>5</sup> They can be calculated with any accuracy for specific values of  $\zeta$  and  $Q$  using mathematical packages (for example, Maple 2016 software package). Spin-wave resonance in the gradient structures of magnetic parameters formed by a convex quadratic potential is studied here for the first time. Spin-wave oscillations in the gradient structures of the potential well, potential barrier, and potential quadratically decreasing from one film surface to another are considered. The calculation was carried out with the same values of the magnetic parameters that were used in Sec. II A.

The convex quadratic potential leads to a fundamental difference between all gradient structures (Fig. 4, red thick dashed curves) from similar structures formed by a concave quadratic potential (Fig. 2, red thick dashed curves). Potential wells entering

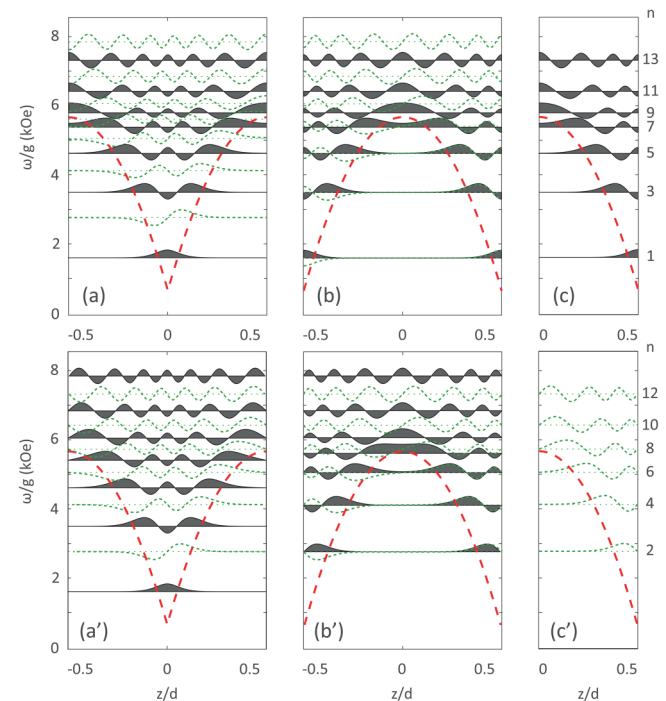


**FIG. 4.** Gradient structures of the effective magnetic field  $H^{\text{eff}}(z)$  described by a convex quadratic function: potential well (a) and (a'), potential barrier (b) and (b'), and monotonic decrease in potential between the surfaces of the film (c) and (c'). The frequencies  $\omega_n$  of discrete levels  $n$  and the waveforms of spin-wave oscillations  $m_n(z)$ . Designations as in Fig. 2.

into all gradient structures sharply narrow, and their bottom is sharpened. The arrangement of the levels of the discrete frequency spectrum  $\omega_n$  changes just as dramatically. The distances between the spectral levels with increasing  $n$  for  $n < n_c$  decrease (Fig. 4) instead of their uniform location for the concave potential (Fig. 2). For  $n > n_c$ , the distance between the levels begins to increase, approaching with increasing  $n$  of the quadratic dependence  $\omega_n(n)$ , as for the concave quadratic potential. As in the case of a concave quadratic potential, degeneration of even and odd levels in the structure of the potential barrier [Figs. 4(b) and 4(b')] occurs, which is removed at  $n > n_c$ .

The main characteristics of the oscillations calculated by us: the discrete frequency spectrum  $\omega_n(n)$  [Figs. 5(e) and 5(e')] and the relative susceptibility  $\chi_n/\chi_1^0$  [Figs. 5(f) and 5(f')] vs  $n$  for the case of a convex quadratic gradient also differ from similar laws for a concave quadratic potential. Susceptibility in Fig. 5 decreases more sharply with increasing  $n$  for  $n > n_c$  than in Fig. 3. In Fig. 5(f'), as in Fig. 3(f'), there are alternating dips and peaks of susceptibility, but a sharper decrease in susceptibility with increasing  $n$  leads to blurring of this effect. The waveform  $m_n(z)$  described by Eqs. (21) and (22) is similar to the waveform described by Eqs. (12) and (13). The increase in the "wavelength" of the oscillations as they approach the surface of the gradient potential, the pinning of their ends on this surface, and the partial tunneling of the oscillations through the surface of the potential can be seen in Figs. 2 and 4.

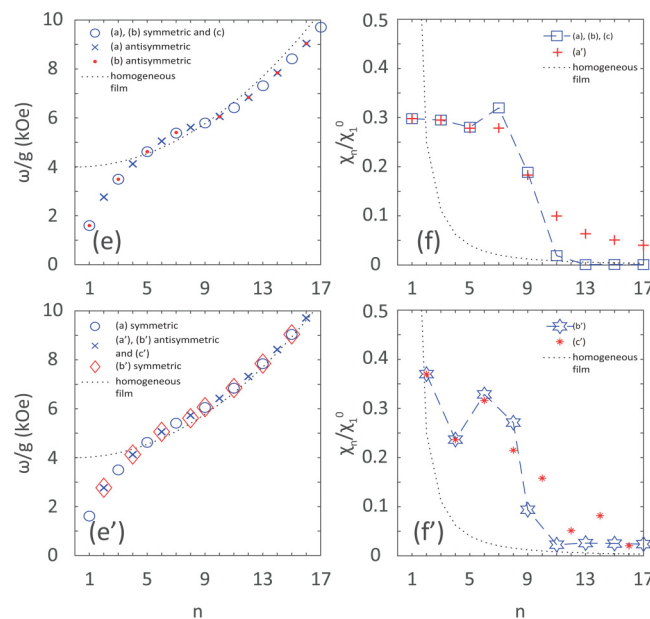


**FIG. 5.** The frequency spectrum  $\omega_n$  (e) and (e') and the relative susceptibility  $\chi_n/\chi_1^0$  (f) and (f') vs  $n$  for unpinning and pinned oscillations, respectively, in the gradient structures of  $H^{\text{eff}}(z)$  described by a convex quadratic function. Designations of the symmetry of oscillations and gradient structures corresponding to them are shown in the figures with links to Figs. 4(a)–4(c) and 4(a')–4(c').

As can be seen from Figs. 5(e) and 5(e'), the points of discrete laws  $\omega_n(n)$  for all the gradient structures shown in Fig. 4 are located along the same continuous curve. This allows us to draw a general conclusion similar to that made in Sec. II A for the case of structures described by a concave quadratic function.

The form of the law  $\omega_n(n)$  is the same for all gradient structures in which potential wells are described by a convex quadratic function, or one side is described by a convex quadratic function and the other is bounded by a vertical line (film surface). The "macroscopic" appearance of the gradient structures containing these potential wells does not matter: it can be a potential well [Figs. 4(a) and 4(a')], a potential barrier [Figs. 4(b) and 4(b')], or a monotonous increasing potential [Figs. 4(c) and 4(c')]. However, the forms of laws for gradient structures described by convex or concave quadratic functions are significantly different. The inflection of the function  $\omega_n(n)$  in the vicinity of  $n = n_c$  occurs for the case of gradient structures described by a convex quadratic function and a smooth bending for the case of a concave quadratic function.

For the confluent hypergeometric Kummer functions of an imaginary argument, there is no such representation as Hermite polynomials for functions of a real argument that would allow us to obtain an analytical expression for the dependence  $\omega_n(n)$  for small  $n$ . Therefore, we selected an analytical expression that would most accurately describe the results of our numerical calculations. As a result, we obtained the laws of the dependence of the oscillation frequency  $\omega_n$  on  $n$  for all structures with a convex quadratic potential gradient: potential well [Figs. 4(a) and 4(a')], potential barrier [Figs. 4(b) and 4(b')], and a monotonously decreasing potential [Figs. 4(c) and 4(c')] in the limiting cases of small and

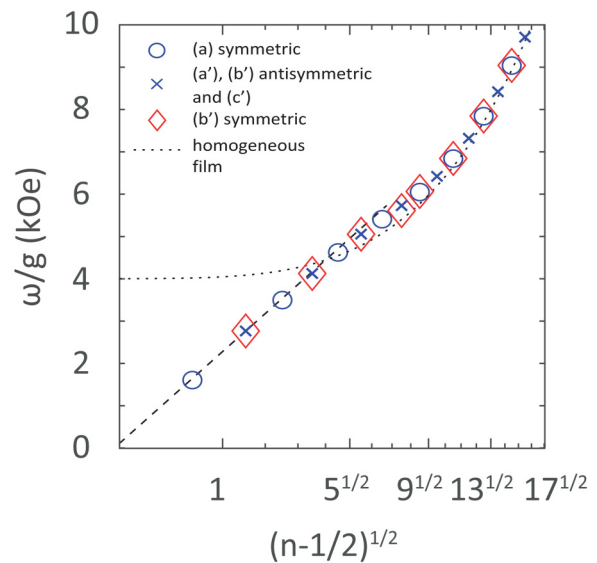


**FIG. 6.** The frequency spectrum  $\omega_n$  of the pinned oscillations vs  $(n - 1/2)^{1/2}$  in the gradient structures of a convex quadratic potential. Designations as in Fig. 5(e').



large  $n$  have the form

$$\omega_n \propto \begin{cases} (n - 1/2)^{1/2}, & n \ll n_c, \\ n^2, & n \gg n_c. \end{cases} \quad (23)$$

Indeed, the numerically found function  $\omega_n$  vs  $(n - 1/2)^{1/2}$  for  $n < n_c$  has the form of a straight line (Fig. 6).

### C. Magnetic anisotropy gradient

The uniaxial magnetic anisotropy  $\beta(z)$ , whose axis is perpendicular to the film surface, is included in Eq. (2) with a plus sign. Therefore, in contrast to the variable magnetization  $M(z)$ , the concave gradient function of the magnetic potential  $H^{\text{eff}}(z)$  corresponds to the concave function  $\beta(z)$ , and the convex function  $H^{\text{eff}}(z)$  corresponds to the convex function  $\beta(z)$ . The quadratic gradient structures corresponding to  $\beta(z)$  are described in the same figure as in Fig. 1 for  $M(z)$ . Formulas for a convex quadratic dependence  $M(z)$ , Eqs. (4)–(6), are replaced by formulas of the form

$$\beta(z) = \beta_{\text{max}} [1 - \varepsilon'(pz)^2], \quad (24)$$

and so on, where

$$\varepsilon' = \Delta\beta/\beta_{\text{max}}, \quad \Delta\beta = \beta_{\text{max}} - \beta_{\text{min}}. \quad (25)$$

For a concave quadratic dependence  $\beta(z)$  in expressions of the form (24),  $\beta_{\text{max}}$  is replaced by  $\beta'_{\text{min}}$ , which corresponds to the minimum of the concave function  $\beta(z)$  and the minus sign in square brackets for the plus sign. All results of Sec. II A for a concave quadratic potential now correspond to a concave quadratic function  $\beta(z)$  and the results of Sec. II B to a convex quadratic function  $\beta(z)$ .

### III. CONCLUSION

The theory of spin-wave resonance in ferromagnetic films with a gradient structure of magnetic parameters described by both concave and convex quadratic functions is developed. Gradient structures such as a potential well, a potential barrier, and a monotonic change in potential between the surfaces of the film are considered (for one of these six structures—a parabolic potential well—the theory of spin-wave resonance was developed previously<sup>6–9</sup>). It is shown that the law of the dependence of the resonance frequency  $\omega_n$  on the spectral level  $n$ , which for the parabolic potential well for  $n < n_c$  has the form  $\omega_n \propto n$ , where  $n_c$  is the level closest to the upper boundary of the gradient potential, is also valid for structures such as the potential barrier and monotonically changing potential if potential wells in these structures are formed by parts of a concave quadratic function and film surfaces. The law of the dependence of the resonance frequency  $\omega_n$  on the spectral level  $n$ , valid for  $n < n_c$  for all three gradient structures (potential well, potential barrier, and monotonic change in potential) formed by a convex quadratic function, was first derived by us numerically and approximated by the analytical function  $\omega_n \propto (n - 1/2)^{1/2}$ . It is shown that the degeneracy of the frequencies of symmetric and antisymmetric oscillations occurs at  $n < n_c$  for structures of the type of potential barriers formed by both concave and convex

quadratic functions. The values of the high-frequency susceptibility of the resonance peaks of all investigated gradient structures at  $n < n_c$  (except for the first peak) are many times higher than the values of the susceptibility peaks of homogeneous films. The laws of the dependence of  $\chi_n$  on  $n$  for  $n < n_c$  are different for different gradient structures and different boundary conditions on the film surface. Thus, an experimental study of the law  $\omega_n(n)$ , the presence or absence of degeneracies of frequencies of oscillations of different symmetries, and the laws  $\chi_n(n)$  in many cases makes it possible to identify the type of a real gradient structure in the sample. The importance of this identification is due to the possibility that any other magnetic parameter may appear during the production of films of an uncontrolled gradient (for example, uniaxial magnetic anisotropy arising due to the magnetoelastic interaction between the layers of the gradient structure).

Spin-wave resonance in gradient magnets is considered in the work with a constant magnetic field  $H$  and a changing frequency  $\omega$ . This allows us to describe the physics of processes in standard terms of discrete spectral levels, gradient potential, etc. Experimental studies of spin-wave resonance are carried out, as a rule, at a constant frequency  $\omega$  and a changing magnetic field  $H$ . The transition from one consideration scheme to another for gradient films does not differ from the same transition for homogeneous films, and the graphs obtained for discrete frequencies obtained in this work can easily be rearranged into graphs for discrete resonant fields. In particular, the limit equations (19) and (23), which describe the dependence of the discrete frequencies  $\omega_n$  on  $n$ , when replacing the minus sign in front of their right sides, describe the laws of decreasing resonant magnetic fields from a certain initial field with increasing resonance number  $n$ .

Theoretical studies of spin-wave resonance in ferromagnetic films with a gradient structure of magnetic parameters, both carried out in this work, and all previous studies<sup>6–11</sup> were built on the basis of Eq. (1), which corresponds to the sample magnetized to saturation. This corresponds to the requirement that the effective magnetic field  $H^{\text{eff}}(z)$  be positive, defined by Eq. (2) for all values of the interval of variation of the  $z$  coordinate in the gradient sample. The first experiments<sup>7</sup> to study spin-wave resonance in films with a predetermined gradient of magnetic parameters were carried out at a frequency of 9.2 GHz. The requirement of positivity of  $H^{\text{eff}}(z)$  under these conditions can be violated for some values of the resonance fields  $H_n$ . The developed theory in this case cannot lead to an agreement with the experiment. A particularly large discrepancy between the theory and experiment is in the case when the resonance fields  $H_n$  are measured at  $\omega = \text{const}$ , since each resonance field  $H^{\text{eff}}$  in an unsaturated sample corresponds to different magnetic states. A way out of this situation would be to conduct experimental studies of gradient films at higher frequencies and, accordingly, in high magnetic fields when the requirement is fulfilled.

The authors hope that this work stimulates the development of technology for the creation and experimental study of such gradient structures in magnetic films, for which the frequency spectrum and high-frequency susceptibility of spin-wave resonances are theoretically calculated. The creation of such materials would contribute to eliminating the lag in the study and application of gradient magnetic materials from similar studies in the field of optical and elastic gradient metamaterials.<sup>1</sup>

## ACKNOWLEDGMENTS

This work was partially supported by the Russian Foundation for Basic Research, Government of Krasnoyarsk Territory, Krasnoyarsk Regional Fund of Science to the research project (No. 18-42-243005) “Synthesis and investigation of magnetic properties of gradient materials that are characterized by predetermined type of the magnetic parameter change” and the Krasnoyarsk Regional Fund of Science in the framework of participation in the conference “VII Euro-Asian Symposium ‘Trends in MAGnetism’ (EASTMAG 2019).”

## REFERENCES

- <sup>1</sup>A. B. Shvartsburg and A. A. Maradudin, *Waves in Gradient Metamaterials* (World Scientific Publishing Co. Pte. Ltd, 2013).
- <sup>2</sup>R. S. Iskhakov, L. A. Chekanova, and I. G. Vazhenina, *Izv. RAN* **77**, 1469 (2013) [*Bull. Russ. Acad. Sci. Phys.* **77**, 1265 (2013)].
- <sup>3</sup>C. Kittel, *Phys. Rev.* **110**, 1295 (1958).
- <sup>4</sup>P. E. Wigen, C. F. Kooi, M. R. Shanabarger, and T. D. Rossingt, *Phys. Rev. Lett.* **9**, 206 (1962).
- <sup>5</sup>M. Abramowitz and I. A. Stegun, *Handbook of Mathematical Functions: With Formulas, Graphs, and Mathematical Tables* (Dover Publications Inc., New York, 1972).
- <sup>6</sup>A. M. Portis, *Appl. Phys. Lett.* **2**, 69 (1963).
- <sup>7</sup>J. T. Davies, *J. Appl. Phys.* **35**, 804 (1964).
- <sup>8</sup>E. Hirota, *J. Phys. Soc. Jpn.* **19**, 1 (1964).
- <sup>9</sup>P. E. Wigen, C. F. Kooi, and M. R. Shanabarger, *J. Appl. Phys.* **35**, 3302 (1964).
- <sup>10</sup>E. Schlomann, *J. Appl. Phys.* **36**, 1193 (1965).
- <sup>11</sup>B. Hoekstra, R. P. van Staple, and J. M. Robertson, *J. Appl. Phys.* **48**, 382 (1977).
- <sup>12</sup>M. Nisenoff and R. W. Terhune, *J. Appl. Phys.* **36**, 732 (1965).
- <sup>13</sup>W. Wang, Z. Jiang, and Y. Du, *J. Appl. Phys.* **78**, 6679 (1995).
- <sup>14</sup>J. Du, J. Wu, L. N. Tong, M. Lu, J. H. Du, M. H. Pan, H. R. Zhai, and H. Xia, *Phys. Status Solidi A* **167**, 183 (1998).
- <sup>15</sup>A. Butera, J. N. Zhou, and J. A. Barnard, *Phys. Rev. B* **67**, 12270 (1999).
- <sup>16</sup>A. Butera, J. N. Zhou, and J. A. Barnard, *J. Appl. Phys.* **87**, 5627 (2000).
- <sup>17</sup>Y. W. Du, H. Sang, Q. Y. Xu, W. N. Wang, and S. Zhang, *Mater. Sci. Eng. A* **286**, 58 (2000).
- <sup>18</sup>T. G. Rappoport, P. Redlinski, X. Liu, G. Zarand, J. K. Furdyna, and B. Janko, *Phys. Rev. B* **69**, 125213 (2004).
- <sup>19</sup>E. Denisova, R. Iskhakov, L. Chekanova, Y. Kalinin, and A. Sitnikov, *Solid State Phenom.* **190**, 466 (2012).
- <sup>20</sup>S. T. B. Goennenwein, T. Graf, T. Wassner, M. S. Brandt, M. Stutzmann, J. B. Philipp, R. Gross, M. Krieger, K. Zurn, P. Ziemann, A. Koeder, S. Frank, W. Schoch, and A. Waag, *Appl. Phys. Lett.* **82**, 730 (2003).
- <sup>21</sup>R. B. Morgunov, M. Farle, and O. L. Kazakova, *Zh. Eksp. Teor. Fiz.* **134**, 141 (2008) [*J. Exp. Theor. Phys.* **107**, 113 (2008)].
- <sup>22</sup>C. Bihler, W. Schoch, W. Limmer, S. T. B. Goennenwein, and M. S. Brandt, *Phys. Rev. B* **79**, 045205 (2009).
- <sup>23</sup>A. I. Dmitriev, R. B. Morgunov, O. L. Kazakova, and Y. Tanimoto, *Zh. Eksp. Teor. Fiz.* **135**, 1134 (2009) [*J. Exp. Theor. Phys.* **108**, 985 (2009)].
- <sup>24</sup>A. I. Dmitriev, O. V. Koplak, and R. B. Morgunov, *Fiz. Tverd. Tela* **54**, 1292 (2012) [*Phys. Solid State* **54**, 1370 (2012)].
- <sup>25</sup>V. A. Ignatchenko and D. S. Tsikalov, “Spin-wave oscillations in gradient ferromagnets: Exactly solvable models,” *J. Magn. Magn. Mater.* (in press) (2020).